Loss of synchronization in lasers via parameter degradation

Carlos L. Pando L.
Instituto de Fisica, Universidad Autónoma de Puebla, Apartado Postal J-48, Puebla, Puebla 72570, Mexico
(Received 13 February 1997)

We have found a general scaling law that describes the loss of forced synchronization in single-mode lasers. The degrading parameters are the corresponding cavity frequencies and the atomic frequencies of the synchronizing lasers. The scaling is general in the sense that it does not depend on the laser operation regime or whether the laser belongs to class *A*, class *B*, or class *C*. [S1063-651X(98)00302-X]

PACS number(s): 05.45.+b, 42.55.−f

I. INTRODUCTION

Synchronization of systems whose dynamics is periodic is an important and well-known effect in physics, engineering, and other disciplines [1,2]. Recently, synchronization of chaos [3] has aroused much interest due to its potential applications [2,4]. In this article we discuss a general scaling law that describes the way forced (unidirectional) synchronization is lost in single-mode lasers as the synchronizing (master) and synchronized (slave) lasers differ more and more in their cavity and atomic frequencies. These lasers can operate in periodic, chaotic, or steady-state regimes.

It is said that two dynamical systems synchronize if the distance between their states converges to zero as time goes to infinity [1,2]. This refers to periodic as well as chaotic synchronization. Synchronization of two laser systems is closely related to laser injection locking [5]. The latter has received a great deal of attention since the invention of the laser [5]. Here the basic idea is to inject a weak monochromatic continuous wave laser signal into the resonant cavity of another laser such that the natural lasing frequencies of both lasers are within a certain locking range. As a result, the lasing frequency of the laser undergoing the injection becomes equal to that of the injected laser signal.

Recently, within the context of chaotic synchronization, different ways to achieve synchronization in laser systems have been carried out [6–11]. In Ref. [6] a model consisting of three semiconductor waveguide lasers is considered. These lasers are coupled by means of their overlapping evanescent fields. Synchronization between two chaotic Nd:YAG lasers (where YAG denotes yttrium aluminum garnet) was achieved experimentally by the overlap of the intracavity laser fields [7]. Synchronization between two chaotic diode resonators has been experimentally carried out by applying a generalization of the occasional proportional feedback scheme [8]. On the other hand, two CO_2 chaotic lasers with saturable absorber were synchronized by injecting the radiation of the master CO_2 laser into the saturable absorber of the slave CO_2 laser [9]. In Ref. [10] a regime of recurrent synchronization is found in CO_2 laser systems, which is further generalized for different dynamical systems.

Another particular case in a system of two lasers consists in optically coupling one laser to the other while leaving one of the lasers uncoupled [11]. This way of synchronization is called forced (unidirectional) synchronization. This is precisely the coupling scheme considered in this article. It must be underlined that, upon unidirectional synchronization of the lasers, the coupling term, which appears in the slave laser model, tends to zero regardless of the laser operation regime. Here the coupling term is proportional to the difference between the electric fields of the coupled lasers.

For the sake of illustration, it is useful to compare the classical Landau theory of second-order phase transitions [12] with the loss of synchronization as studied in this paper. In the classical Landau theory of second-order phase transitions, a system undergoes a transition from one phase (state) to another one in a continuous way. Here the symmetry of one phase is higher than that of the other and it is precisely the symmetry of the system that changes discontinuously at the transition point [12]. As a result, it is possible to find that the degree of ordering η, a quantity that depends on the state of the system, depends, as a power law, on the difference between the current value of the external parameter and its critical value, where the value $\eta=0$ corresponds to the most symmetric phase [12]. Along similar lines we can consider the loss of unidirectional synchronization. The state of (perfect) synchronization is characterized by the symmetry relation $F_i^{(\mathrm{master})}=F_i^{(\mathrm{slave})}$, where $F_i^{(\mathrm{master,slave})}$ stand for the variables of the master and slave lasers, respectively. As long as the corresponding frequencies of the master and slave lasers are different, this symmetry is broken. Here the degree of ordering η is a suitable distance between the states of both lasers, while the difference between the external parameter and its critical value is given by a suitable distance between the frequencies of both lasers in parameter space. Here η depends, as a power law, on the distance between the frequencies of the lasers, as we will see. For lasers in a steady state, we demonstrate this property analytically and numerically, while for lasers in a time-dependent state, this is shown numerically. Here also $\eta=0$ corresponds to the symmetric state, i.e., the state of (perfect) synchronization.

In contrast, there are interesting studies dealing with loss of synchronization in blowout bifurcations [13]. Here, assuming always that the parameters of the synchronizing systems are the same, it was shown that there is an interval of the coupling constant(s) where synchronization is lost [13]. At the boundary of this interval, synchronous chaotic behavior is interrupted by bursts of desynchronized motion [13]. In contrast to Ref. [13], the system that we study here can be considered as made of two stages. First, both the master and slave lasers reach the state of (perfect) synchronization since the (unidirectional) coupling constant has been made large

enough. At this stage, all the parameters of both lasers are the same, with the exception of the coupling that affects only the slave laser. Second, once (perfect) synchronization is reached, we allow a progressive smooth variation of the parameters of the lasers. In the present case, we change the cavity frequency, the atomic frequency, or both frequencies of the master laser, leaving those of the slave laser unchanged. We can change the frequencies of the slave laser leaving those of the master laser unchanged. That yields the same result.

Finally, it is worth mentioning that for chaotic maps and flows, Ref. [14] studies the degradation (loss) of synchronization as the parameters of the synchronizing systems diverge. This study [14] used the scheme of Pecora and Carroll [3], which is impossible to implement in lasers to reach synchronization via optical coupling [7]. In Ref. [14] mutual correlation dimensions were found to scale with the difference between corresponding parameters of the synchronizing systems. In this study, no comment was made regarding the universality of the scaling exponents for a given mutual correlation dimension [14]. In contrast, our model is based on the forced synchronization scheme, which can be implemented naturally in laser systems via all-optical methods. The power-law scaling found in the extended Lorenz model is general for all the laser operation regimes and all the different relaxation rates of this laser model. The latter defines the different types of lasers.

This article is divided as follows. In Sec. II we study the loss of synchronization in unidirectionally coupled Hopf oscillators. In Sec. III we describe the unidirectionally coupled extended Lorenz model. In Sec. IV we consider the loss of synchronization in the extended Lorenz model. In Sec. V we give the conclusions.

II. LOSS OF SYNCHRONIZATION IN UNIDIRECTIONALLY COUPLED HOPF OSCILLATORS

Before considering the loss of synchronization in the extended Lorenz model, we will present a simple model that illustrates how the above-mentioned power-law arises. The model is given by

$$\frac{dZ_k}{dt}=Z_k(-|Z_k|^2+\alpha_k)+\Gamma_k(Z_l-Z_k). \tag{1}$$

Here Z_k and Z_l are the complex amplitudes of the Hopf oscillators, where $k=m,s$ and $l=s,m$, respectively. m and s stand for the master and slave oscillators, respectively. Here, without loss of generality, $\alpha_m=1+i\omega_m$ and $\alpha_s=1+\mu+i\omega_s$. To consider only unidirectional coupling, we need to set $\Gamma_s\equiv\Gamma$ and $\Gamma_m=0$. Using the new variables $Z_m=\rho_m\exp(i\theta_m)$ and $Z_s=\rho\exp(i\theta)$, we obtain for the slave oscillator

$$\frac{d\rho}{dt}=\rho(1+\mu-\rho^2)+\Gamma(\rho_m\cos\chi-\rho),$$

$$\frac{d\chi}{dt}=\delta-\Gamma\frac{\rho_m}{\rho}\sin\chi, \tag{2}$$

where $\chi\equiv\theta_m-\theta_s$ and $\delta=\omega_m-\omega_s$. The master oscillator Z_m describes a regular oscillation with $\rho_m=1$ and $d\theta_m/dt=\omega_m$. The onset of this regular oscillation occurs as a result of a supercritical Hopf bifurcation. The locking range is defined by the equation $d\chi/dt=0$ [2,5]. Locking between the master and slave oscillators is lost through a saddle-node bifurcation [2]. As a result, within the locking range, the (instantaneous) frequency of the slave oscillator becomes the same as that of the master $d\theta/dt=\omega_m$. Within the locking range ρ_m and ρ will differ from each other unless $\delta=0$ and $\mu=0$.

Let us first consider the case $\mu=0$ and $\delta\ll\Gamma$. From Eq. (2) we obtain

$$\sin\chi=\frac{\delta}{\Gamma}\rho,$$

$$\cos\chi\approx1+\frac{1}{2}\left(\frac{\delta}{\Gamma}\rho\right)^2+O(\rho^4)>0. \tag{3}$$

Next, in order to find the steady-state solution for ρ, we insert in Eq. (2) the approximate expression for $\cos\chi$ and expand ρ in series of $\epsilon\equiv\frac{1}{2}(\delta/\Gamma)^2\ll1$. As a result, we obtain

$$\rho=1+\frac{\Gamma}{2+\Gamma}\epsilon+\frac{\Gamma^2(4-\Gamma)}{(2+\Gamma)^3}\epsilon^2+O(\epsilon^3). \tag{4}$$

Therefore, as δ undergoes small changes within the full locking range, the power-law scaling for ρ is given by

$$\ln|\rho-\rho_m|\approx2\ln|\delta|+C, \tag{5}$$

where C is a constant. Thus the scaling exponent is given by $\nu=2$. Equation (5) describes the loss of forced synchronization in the coupled Hopf oscillators.

Now let us consider the case $\mu\ll1$ and $\delta=0$. Here the locking condition is always satisfied and $\chi=0$. The equation for ρ is given by

$$\rho=1+\frac{1}{2+\Gamma}\mu+O(\mu^2). \tag{6}$$

Thus, as μ undergoes small changes, $\rho-\rho_m\sim\mu$ and the exponent is $\nu=1$. We will show below that the exponents $\nu=1,2$ considered above are related as well to the scaling of amplitudes, i.e., bounded variables of the extended Lorenz model when the corresponding atomic and cavity frequencies of the lasers differ from each other.

We underline that Eq. (1) can be derived from the extended Lorenz model upon adiabatic elimination of the atomic variables and neglecting the frequency pulling and pushing coefficients [15]. The Hopf oscillator model describes the transversally and longitudinally monomode He-Ne laser oscillating at 3.39 μm [16].

III. THE MODEL OF THE LASER SYSTEM

We will assume that the laser systems are coupled similarly to the Hopf oscillators, i.e., unidirectionally. This way of coupling in lasers can be realized with all-optical methods [5,7,11,17]. When (perfect) synchronization between both master and slave lasers is reached, the synchronization (cou-

pling) term vanishes and the equations of both lasers become the same.

We now introduce the model for the laser system where a finite detuning between the atomic transition frequency ω_a of the resonant levels and the cavity frequency ω_c is present. The model is known as the extended Lorenz model [18,19]. It is based upon the usual field-matter equations for two-level atoms in a resonant cavity [20]. The slave laser system is described by the set of equations

$$\frac{dE}{dt} = -kE + i(\Omega - \omega_c)E - gP + \Gamma k(E_m - E),$$

$$\frac{dP}{dt} = -\gamma_\perp P + i(\Omega - \omega_a)P - gEN,$$

$$\frac{dN}{dt} = g(PE^* + EP^*) - \gamma N + \gamma Q, \tag{7}$$

where E is the complex amplitude of the electric field, P is the polarization, and N is the population difference of the upper and lower resonant energy levels. E_m is the amplitude of the electric field of the master laser. g is the field-matter coupling constant (a real number) and Ω is the frequency of the laser reference frame. Q is the incoherent pump and the relaxation rate of N is written as γ. A similar equation holds for the master laser, except that $\Gamma = 0$ and the atomic transition frequency ω_a^m of the resonant levels and the cavity frequency ω_c^m can be different from those of the slave laser.

If we write the electric field and polarization of the slave and master lasers in polar coordinates $E = \rho \exp(i\theta)$, $P = \mu \exp(i\psi)$, $E_m = \rho_m \exp(i\theta_m)$, and $P_m = \mu_m \exp(i\psi_m)$, the slave laser equations become

$$\frac{d\rho}{dt} = -\beta\rho - \sqrt{\beta}\mu \cos\delta + \beta\Gamma(\rho_m \cos\chi - \rho),$$

$$\frac{d\mu}{dt} = -\mu - \sqrt{\beta}\rho N \cos\delta,$$

$$\frac{d\delta}{dt} = \Delta + \sqrt{\beta}\left[\frac{\mu}{\rho} + N\frac{\rho}{\mu}\right]\sin\delta + \beta\Gamma\frac{\rho_m}{\rho}\sin\chi,$$

$$\frac{dN}{dt} = 4\sqrt{\beta}\mu\rho\cos\delta - \gamma N + \gamma Q,$$

$$\frac{d\chi}{dt} = \frac{\omega_c - \omega_c^m}{\gamma_\perp} + \sqrt{\beta}\left[\frac{\mu_m}{\rho_m}\sin\delta_m - \frac{\mu}{\rho}\sin\delta\right] - \beta\Gamma\frac{\rho_m}{\rho}\sin\chi. \tag{8}$$

Here $\beta = k/\gamma_\perp$, $\Delta = (\omega_a - \omega_c)/\gamma_\perp$, and $\delta = \theta - \psi$. t, ρ, and μ have been renormalized as $t \to \gamma_\perp t$, $\rho \to g\rho/\sqrt{k\gamma_\perp}$, and $\mu \to g^2\mu/k\gamma_\perp$, respectively. N and Q are renormalized in the same way as μ. The subscript or superscript m labels variables or parameters of the master laser. The phase θ influences the dynamics of the slave laser model via the equation for $\chi \equiv \theta_m - \theta$. The same equation holds for the master laser, except that there $\Gamma = 0$ and the phase θ_m does not influence the dynamics of the master laser model.

When $\Gamma = 0$, the master and slave lasers are uncoupled. The dynamics of these systems has been studied extensively in previous articles [18,19]. In this case, at a steady state $\dot{\theta}(t) = 0$ and the frequency Ω_0 of the reference frame is given by the well-known relation

$$\Omega_0 = \frac{\omega_c\gamma_\perp + \omega_a k}{\gamma_\perp + k}. \tag{9}$$

For the sake of definition, we have set Ω equal to the lasing frequency at a steady state Ω_0 in both the master and slave lasers. We define $\Delta_m = (\omega_a^m - \omega_c^m)/\gamma_\perp$ and $\Delta = (\omega_a - \omega_c)/\gamma_\perp$ as the detunings in each laser system. If in the extended Lorenz model the relaxation rates of the atomic variables differ substantially, particular cases can be derived from this model that have been used to describe important lasers such as CO_2, Nd:YAG, and He-Ne lasers [20].

IV. DEGRADATION OF SYNCHRONIZATION IN LASERS WITH DIFFERENT DYNAMICAL REGIMES

A. Steady-state operation

By increasing the pump Q from a state with $\rho_m = 0$, the extended Lorenz model undergoes eventually a transcritical bifurcation and reach a steady state with nonzero amplitude $\rho_m \neq 0$. When the instantaneous laser frequencies $d\theta_m/dt$ and $d\theta/dt$ are the same, this defines, as before, the locking range for lasers at a steady state, i.e., $d\chi/dt = 0$. Here we consider two cases: (a) the case when the cavity frequencies of both lasers are the same, i.e., $\omega_c = \omega_c^m$, and (b) the case when the atomic frequencies of both lasers are the same, i.e., $\omega_a = \omega_a^m$.

When $\omega_c = \omega_c^m$, we obtain, from the locking condition $d\chi/dt = 0$,

$$\beta\Gamma\frac{\rho_m}{\rho}\sin(\chi) = \sqrt{\beta}\left[\frac{\mu_m}{\rho_m}\sin(\delta_m) - \frac{\mu}{\rho}\sin(\delta)\right]. \tag{10}$$

Subtracting the equation for $d\delta/dt$ from that for $d\delta_m/dt$ in the laser model and making use of Eq. (10) yields

$$\sqrt{\beta}\left[N_m\frac{\rho_m}{\mu_m}\sin(\delta_m) - N\frac{\rho}{\mu}\sin(\delta)\right] + \epsilon = 0, \tag{11}$$

where $\epsilon = \omega_a^m - \omega_a$, $|\epsilon| \ll 1$, is the perturbation parameter. In a steady state, it is possible to represent the difference between the variables, i.e., amplitudes of the master and slave lasers, as a Taylor expansion in terms of ϵ over a range of small detunings δ. Therefore, the linear term coefficient of ϵ in these Taylor expansions is in general different from zero in order to satisfy Eq. (11) and as a result the scaling exponent is one.

On the other hand, when $\omega_a = \omega_a^m$, we obtain from the locking condition $d\chi/dt = 0$

$$\beta\Gamma\frac{\rho_m}{\rho}\sin(\chi) = \sqrt{\beta}\left[\frac{\mu_m}{\rho_m}\sin(\delta_m) - \frac{\mu}{\rho}\sin(\delta)\right] + \epsilon, \tag{12}$$

where this time $\epsilon = \omega_c - \omega_c^m$, $|\epsilon| \ll 1$. It is easy to check that the equality $\delta_m = \delta$ holds. This is shown by using the equation for $d\mu/dt = 0$ and the equation

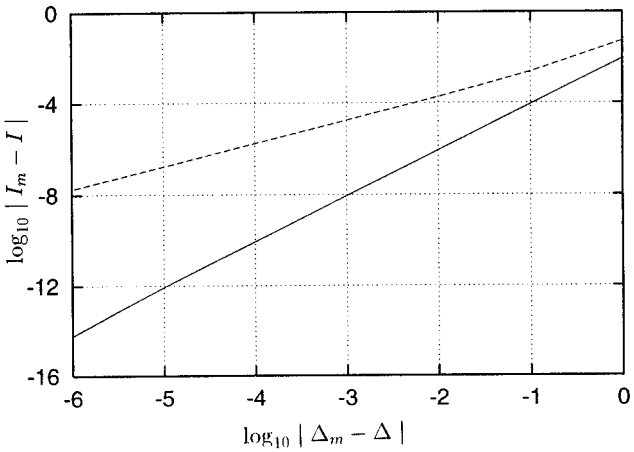

FIG. 1. Plot of $\log_{10}|I_m - I|$ versus $\log_{10}|\Delta_m - \Delta|$. The solid line stands for the case $\omega_a^m = \omega_a$, while the dashed line stands for the case $\omega_c^m = \omega_c$, Here the laser operates at steady state with a coupling constant $\Gamma = 2.0$.

$$\sqrt{\beta}\left[N_m \frac{\rho_m}{\mu_m} \sin(\delta_m) - N \frac{\rho}{\mu} \sin(\delta) \right] = 0, \tag{13}$$

which was obtained similarly to Eq. (11). By representing the other variables of the slave laser as a Taylor expansion in terms of ϵ and keeping the linear terms in Eq. (8), we obtain

$$\begin{aligned} (1+\Gamma)\beta\rho_1 + \sqrt{\beta}\cos(\delta)\mu_1 + \beta\Gamma\rho_m[1-\cos(\chi)]\epsilon^{-1} = 0, \\ \sqrt{\beta}N_m \cos(\delta)\rho_1 + \mu_1 + \sqrt{\beta}\rho_m \cos(\delta)N_1 = 0, \\ 4\sqrt{\beta}\mu_m \cos(\delta)\rho_1 + 4\sqrt{\beta}\rho_m \cos(\delta)\mu_1 - \gamma N_1 = 0, \end{aligned} \tag{14}$$

where ϵ has been factored and ρ_1, μ_1, and N_1 are the linear term coefficients in the Taylor expansion. Since ϵ is the perturbation parameter, from Eq. (12) it follows that $\chi \sim \epsilon$. Therefore, in Eq. (14) the factor $1-\cos\chi \sim \chi^2 \sim \epsilon^2$. As a result, the linear equation for the coefficients ρ_1, μ_1, and N_1 becomes homogeneous since terms of order ϵ are not present in this equation. Since the determinant of this linear equation is given by

$$\begin{aligned} &-4\beta^2\rho_m^2 \cos^2(\delta_m)[1+\Gamma+N_m \cos^2(\delta_m)] \\ &-\gamma\beta[1+\Gamma-N_m \cos^2(\delta_m)], \end{aligned} \tag{15}$$

which is in general different from zero, the coefficients ρ_1, μ_1, and N_1 are zero. If the Taylor expansion in Eq. (8) takes into account quadratic terms $\sim\epsilon^2$, the resulting linear equation for the coefficients of the quadratic terms will be inhomogeneous due precisely to the factor $1-\cos\chi$. That is why in the case $\omega_a = \omega_a^m$ the scaling exponent is 2.

Next we will verify numerically the power-law scaling found above. The steady state is defined by the set of parameters $\beta = 2.0$, $\gamma = 0.25$, $Q = 2.0$, and $\Delta = 0.6$. The control parameter is Δ_m. In Fig. 1 we can observe the scaling of the intensity difference between the master and slave laser $I_m - I$ with respect to the mismatch $\Delta_m - \Delta$. $I_m = \rho_m^2$ and $I = \rho^2$. The solid line stands for the case $\omega_a^m = \omega_a$ where only the cavity frequency ω_c^m changes. On the other hand, the dashed line represents the case with $\omega_c^m = \omega_c$ and therefore only ω_a^m changes. In the case $\omega_a^m = \omega_a$, the numerical calculation of the scaling exponent gives $\nu = 2.0 \pm 0.01$, while in the case $\omega_c^m = \omega_c$ it is given by $\nu = 1.0 \pm 0.01$. The scaling for the difference between other corresponding variables of the master and slave lasers, such as that of the populations $N_m - N$ or that of the laser intensity of the electric field $|E_m - E|^2$, shows the same scaling exponents of $I_m - I$.

B. Class-*C* laser operation

When the solution in the Lorenz model is time dependent, the locking condition $d\chi/dt = 0$ no longer holds since the parameters of the master and slave lasers are different. However, the same scaling law discussed above is found here for suitable averages of the difference between the variables, i.e., amplitudes of the master and slave lasers, as we will see below. In a class-*C* laser, the variables of the system that take into account the population inversion and polarization play an important role in the dynamics of the system [20,18,19]. For the parameters $\beta = 2.0$, $\gamma = 0.25$, and $Q = 15.0$, the dynamics and bifurcations of this system have been extensively studied in Refs. [18,19]. Here we set the detuning $\Delta = 0.6$. As before, the control parameter is Δ_m. For these parameters the master oscillator describes chaotic motion [19].

Before we proceed to describe loss of synchronization when the dynamics is chaotic, we will consider the case of (perfect) chaotic synchronization between the master and slave lasers. When the frequencies of both lasers are the same ($\omega_{a,c}^m = \omega_{a,c}$), in order to reach synchronization it is required that the tendency for exponential separation of two close trajectories, one of which belongs to the master laser and the other to the slave laser, must be compensated by the effect of coupling between the lasers. Mathematically, this can be expressed by saying that the largest conditional Lyapunov exponent must be negative in order to reach chaotic synchronization [3,21]. In Fig. 2(a) we can observe the two largest conditional Lyapunov exponents as the coupling constant Γ increases. At $\Gamma_c \approx 0.25$ the master and slave lasers synchronize and as a result the maximum conditional Lyapunov exponent is negative. Another useful quantity to study synchronization is the distance between the states of both lasers. This can be observed in Fig. 2(b), where the dependence of $\log_{10}|1-m|$ and $\log_{10}\sigma$ versus the coupling constant Γ is plotted. m is the slope in the linear regression of the set of points (I_m, I) and σ is its deviation. When $|1-m| \to 0$ and $\sigma \to 0$ (perfect) synchronization sets in, i.e., a straight line with slope one appears in the plane (I_m, I). Both $\log_{10}|1-m|$ and $\log_{10}\sigma$ show a bound of order -13 due to roundoff errors for $\Gamma > \Gamma_c \approx 0.25$. Once the regime of (perfect) chaotic synchronization is reached for a given set of parameters, we start to change $\omega_c^m - \omega_c$, $\omega_a^m - \omega_a$, or both.

We consider now the case $\omega_a^m = \omega_a$. In Fig. 3(a) we can observe the scaling of $\log_{10}|1-m|$ as a function of $\log_{10}|\Delta_m - \Delta| = \log_{10}|\omega_c^m - \omega_c|$ for different values of the coupling constant Γ such that $\Gamma > \Gamma_c \sim 0.25$. In this figure, when $\log_{10}|\Delta_m - \Delta| \sim -6$ or less, scaling is not observed due again to roundoff errors. A related scaling can be observed in Fig. 3(b) for the plot of $\log_{10}\sigma$ versus $\log_{10}|\Delta_m - \Delta| = \log_{10}|\omega_c^m - \omega_c|$. m and σ are calculated from the linear regression of the set of points (I_m, I). Notice that σ accounts

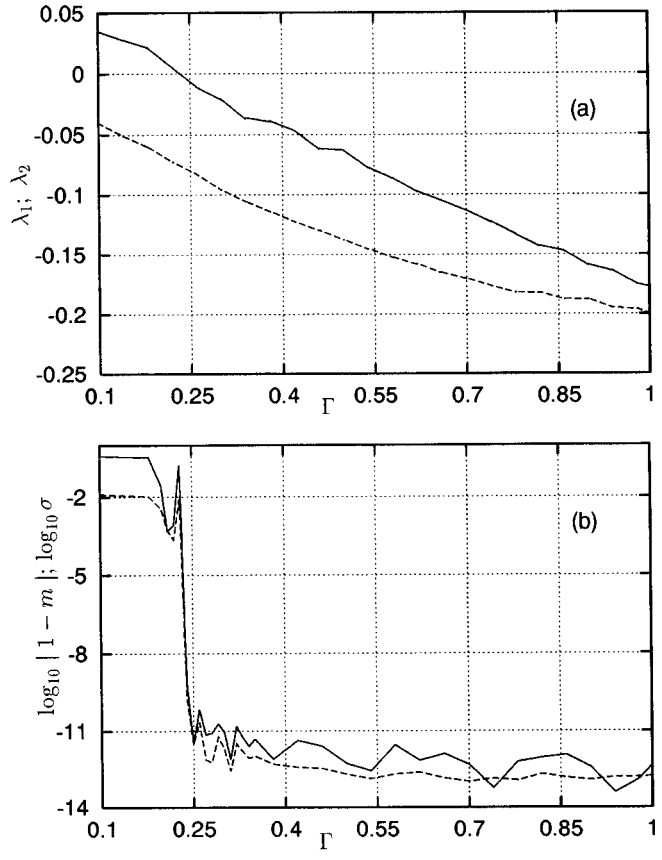

FIG. 2. Here we consider the case with $\omega_a^m=\omega_a$ and $\omega_c^m=\omega_c$ for the class-*C* laser studied in the text. (a) The first two conditional Lyapunov exponents versus the coupling constant Γ. (b) $\log_{10}|1-m|$ and $\log_{10}\sigma$ versus the coupling constant Γ. Here m and σ are the slope and its deviation, respectively, in the linear regression of the set of points (I_m,I). Here and below the solid and dashed lines correspond to the first and second plot, respectively.

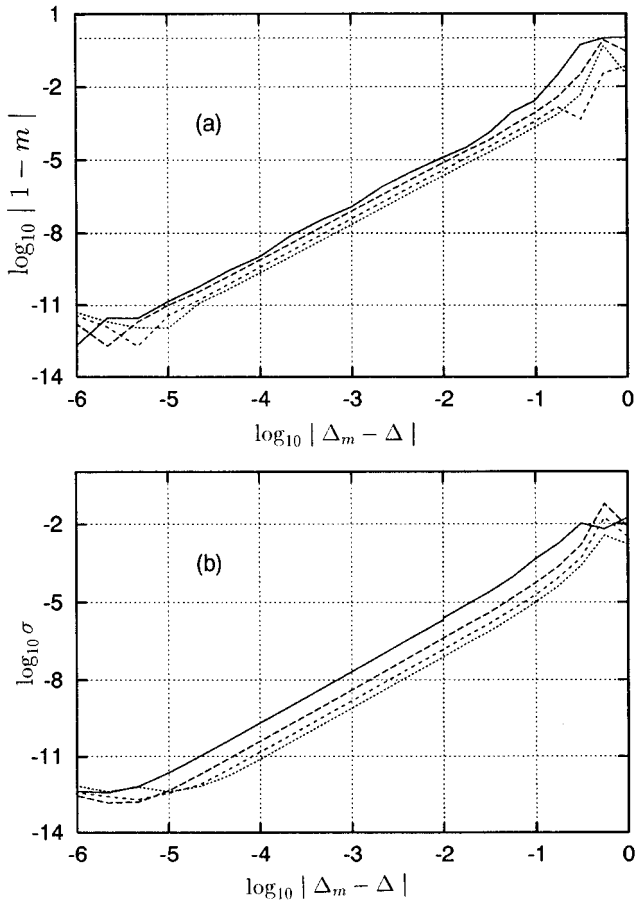

FIG. 3. Here the case $\omega_a^m=\omega_a$ is considered. The parameters correspond to the class-*C* laser. (a) Plot of $\log_{10}|1-m|$ versus $\log_{10}|\Delta_m-\Delta|$ for different coupling constants $\Gamma=0.5$, 1.0, 1.5, and 2.0. (b) Same as (a), but for the corresponding deviation σ. Here the slope m and its deviation σ are calculated as in Fig. 2(b).

for a statistical difference with respect to some optimal fitting straight line with slope m. This suggests that we can find the same scaling in $\log_{10}|\langle I_m-I\rangle|$ and $\log_{10}\sigma(I_m-I)$ versus $\log_{10}|\Delta_m-\Delta|$ where $\langle I_m-I\rangle$ and $\sigma(I_m-I)$ stand for the statistical average and standard deviation, respectively, of the set of points I_m-I. This is confirmed by Figs. 4(a) and 4(b) for different values of the coupling constant Γ, for which $\Gamma>\Gamma_c$. We underline that other averages such those of $F(\rho_m,\mu_m,\delta_m,N_m)-F(\rho,\mu,\delta,N)$, where F is a suitable function, obey the same scaling law.

In Figs. 3 and 4 we have studied the case $\omega_a^m=\omega_a$ for which the scaling exponent is $\nu=2.0\pm0.01$. In contrast, the case $\omega_c^m=\omega_c$ has as scaling exponent $\nu=1.0\pm0.01$. This is shown in Fig. 5 for $\log_{10}\sigma$ versus $\log_{10}|\Delta_m-\Delta|$, where σ is the deviation of the corresponding slope m in the linear regression of the set of points (I_m,I). A similar picture is obtained for the scaling of $\log_{10}|1-m|$. The solid and dashed lines correspond to different coupling constants Γ for which $\Gamma>\Gamma_c$.

Here we give a qualitative explanation to understand why the amplitude scaling in the steady-state case still persists in the chaotic regime or, as we will see, in the periodic regime. One must consider two facts. First, the time average from time derivatives of bounded quantities, i.e., amplitudes, such as ρ, is zero. Second, the time average of the difference between the corresponding amplitudes of the master and slave lasers must have a dependence on the frequencies mismatch that is the same as that of the steady-state case, as long as χ is bounded. As a result, the scaling of the difference of the corresponding averaged amplitudes gives exponents $\nu=1,2$ as explained above.

C. Class-*B* and class-*A* laser operation

The parameters of the class-*C* laser model considered above have been used to describe the dynamics of the NH_3 far-infrared single-mode laser [18]. Class-*B* lasers are systems such as the CO_2 and Nd:YAG lasers. Models for these lasers have been derived as particular cases from the extended Lorenz model [20]. These models are obtained by eliminating adiabatically the atomic polarization P. For class-*A*lasers such as the He-Ne lasers, the polarization P and inversion N can be adiabatically eliminated in the extended Lorenz model [20].

The class-*B*laser model considered here has the set of parameters $\beta=0.0578$, $\gamma=0.0084$, $\Delta=0.6$, and a modulated external pump $Q=1.4\times[1.0+m\ \sin(\omega t)]$. For $m=0.25$ and $\omega=10^{-3}$ (which corresponds to 400 kHz), the laser shows chaotic behavior. For the case $\omega_a^m-\omega_a=0$, the scaling exponent is given by $\nu=2.0\pm0.01$. On the other hand, for the

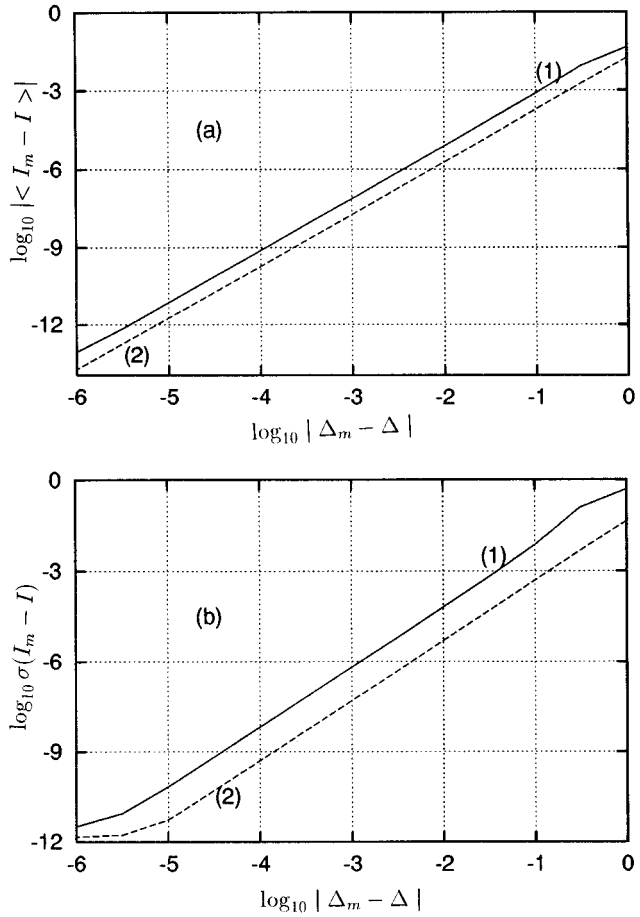

FIG. 4. Here the parameters are the same as in Fig. 3. (a) Plot of $\log_{10}|\langle I_m - I\rangle|$ versus $\log_{10}|\Delta_m - \Delta|$. (b) Plot of $\log_{10}\sigma(I_m - I)$ versus $\log_{10}|\Delta_m - \Delta|$. $\langle I_m - I\rangle$ and $\sigma(I_m - I)$ are the mean and standard deviations, respectively, of the set of data $I_m - I$. The solid line corresponds to $\Gamma = 1.0$, while the dashed line stands for $\Gamma = 2.0$.

case $\omega_c^m - \omega_c = 0$, $\nu = 1.0 \pm 0.01$. A class-*B* laser with modulated losses shows the same scaling laws as the previous cases. Pump-modulated and loss-modulated lasers have been studied theoretically and experimentally [5,22].

For the class-*A* laser model considered here, we have chosen the parameters $\beta = 0.0578$, $\gamma = 0.2$, and $Q = 1.4 \times [1.0 + m \sin(\omega t)]$. Here $m = 0.1$ and $\omega = 0.1$. Under pump modulation, the oscillations in this system are only periodic since the phase space of the system becomes two dimensional. For both cases $\omega_a^m = \omega_a$ and $\omega_c^m = \omega_c$, the same scaling exponents ν found previously hold also here.

D. Simultaneous variation of the cavity frequency and atomic frequency

In the previous subsections we have considered strictly only two cases, namely, $\omega_a^m = \omega_a$ and $\omega_c^m = \omega_c$. Different laser operation regimes, which belong to the same case, have the same scaling exponent. Now we will approach the (perfect) synchronized state by reducing simultaneously the finite detunings $\omega_a^m - \omega_a \neq 0$ and $\omega_c^m - \omega_c \neq 0$ towards zero. This can be carried out by introducing the variables ψ and d:

$$\omega_a^m - \omega_a = d \sin \psi,$$

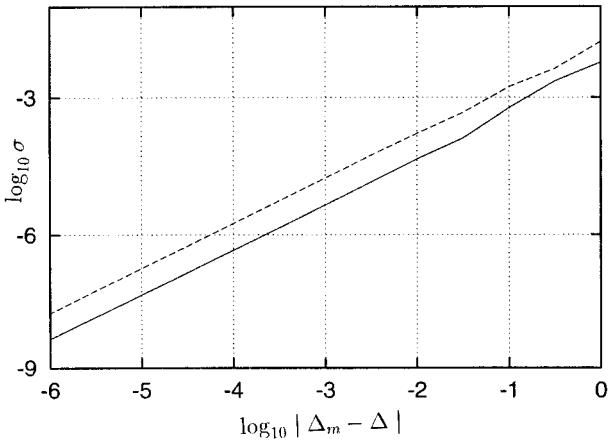

FIG. 5. Here the case $\omega_c^m = \omega_c$ is considered. The parameters correspond to those of the class-*C* laser. Plot of $\log_{10}\sigma$ versus $\log_{10}|\Delta_m - \Delta|$. The solid line stands for $\Gamma = 1.0$ and the dashed line for $\Gamma = 1.5$. σ is the deviation of the best-fitting slope in the linear regression of the set of points (I_m, I).

$$\omega_c^m - \omega_c = d \cos \psi. \tag{16}$$

The corresponding scaling exponents are found by changing d while keeping ψ constant. With this notation, the cases $\omega_a^m - \omega_a = 0$ and $\omega_c^m - \omega_c = 0$ correspond to $\psi = 0, \pi$ and $\psi = \pi/2, 3\pi/2$, respectively.

The scaling exponents ν have been obtained for $\log_{10}|\langle I_m - I\rangle|$ with respect to d. For the steady-state case, $\log_{10}|\langle I_m - I\rangle|$ degenerates into $\log_{10}|I_m - I|$.

Here the parameters of the steady state in the Lorenz model are the same as that of Sec. IV A. In Fig. 6 we see that the scaling exponent is $\nu = 1.0 \pm 0.01$ everywhere with the exception of the vicinity of $\psi = 0$ or π. In Fig. 7(a) we show the slopes ν corresponding to values of ψ for which $\psi \to 0$. In this figure, lines (1) and (2) stand for $\Gamma = 1.0$ and 2.0, respectively, both for $\psi > 0$, while lines (3) and (4) stand for $\Gamma = 1.0$ and 2.0, respectively, both for $\psi < 0$. There is no symmetry between the positive and negative values of ψ. However, as observed in Fig. 7(b) in this vicinity of ψ, the deviation σ of the slope ν is relatively large. This means that in an interval of this vicinity, we cannot characterize the dependence of $\log_{10}|I_m - I|$ on the considered values of d as

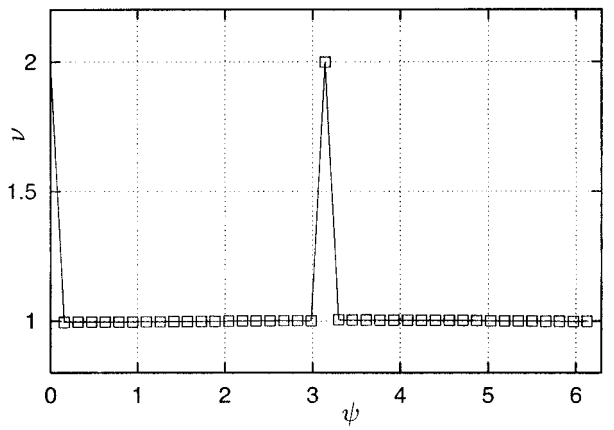

FIG. 6. Plot of the scaling coefficient ν versus the angle ψ (defined in the text). This plot corresponds to the steady-state case.

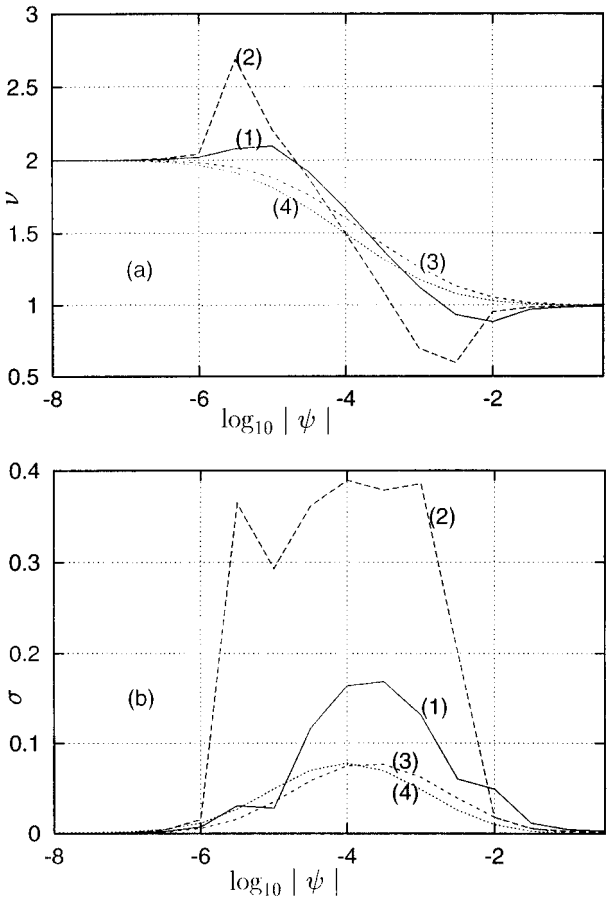

FIG. 7. (a) Plot of the slope coefficient ν versus $\log_{10}|\psi|$ for the steady-state case. Lines (1) and (2) correspond to $\psi>0$ and lines (3) and (4) to $\psi<0$. Lines (1) and (3) are calculated for $\Gamma=1.0$ and lines (2) and (4) for $\Gamma=2.0$. (b) Same as (a), but for the deviation σ of the slope ν.

a certain straight line since consideration of quadratic terms of d is necessary. Here Eq. (11) is replaced by

$$\sqrt{\beta}\left[N_m\frac{\rho_m}{\mu_m}\sin(\delta_m)-N\frac{\rho}{\mu}\sin(\delta)\right]+d\,\sin(\psi)=0. \tag{17}$$

The difference between the corresponding variables of the master and slave lasers can be expressed as a Taylor expansion in terms of d. By the same arguments given in Sec. IV A, the linear term coefficient in these Taylor expansions is in general different from zero as long as $\psi\neq 0$. That is, as $\psi\to 0$ and for small enough values of d, the linear term will be the relevant term. However, as d becomes larger than ψ, the quadratic term becomes more and more relevant. This is precisely what we see in Fig. 7, where ν and σ have been calculated for $10^{-6}\leqslant d\leqslant 10^{-2}$. Within this interval of d and for intermediate values of ψ the dependence of $\log_{10}|I_m-I|$ on d is neither a straight line ($\nu=1$ and $\sigma=0$) nor a parabolic curve ($\nu=2$ and $\sigma=0$) since both terms are relevant. This is the reason for the relative large values σ in this interval of ν.

A similar situation takes place when the trajectory of the laser is chaotic. Here the parameters are the same as those of Sec. IV B. Here the picture is qualitatively the same as that of Figs. 6, 7(a), and 7(b).

V. CONCLUSIONS

In this article we have studied the progressive loss of (perfect) synchronization as the frequencies of the master and slave lasers differ from each other. We have found that the dependence of the distance or average distance between the corresponding amplitudes of both lasers with respect to a small difference in the frequencies between the lasers is ruled by a scaling law. The scaling exponent is generically $\nu=1.0$; however, the scaling exponent becomes $\nu=2.0$ in the case $\omega_a^m-\omega_a=0$. The generality of the scaling exponents for coupled single-mode lasers, which are described by the extended Lorenz model, refers to the fact that the scaling exponents are the same regardless of the type of laser (class *A*, class *B*, or class *C*) and the laser operation regime (steady state, periodic, or chaotic).

It would be interesting to study further the loss of synchronization via parameter degradation in other important laser models such as those of multimode semiconductor and fiber lasers. The extension of these studies to spatially extended laser systems may also be of interest due to the importance in the control of the spatial laser characteristics.

ACKNOWLEDGMENTS

I would like to thank Itamar Procaccia for several important comments. I wish to also thank Raj Roy and his group for useful discussions. I am grateful for support from the Instituto de Física of the UAP. This work was also supported by CONACYT, Mexico.

[1] A. A. Andronov, A. A. Vitt, and S. E. Khaikin, *Theory of Oscillators* (Pergamon, Oxford, 1966).
[2] S. H. Strogatz, *Nonlinear Dynamics and Chaos* (Addison-Wesley, Reading, MA, 1994).
[3] L. M. Pecora and T. L. Carroll, Phys. Rev. Lett. **64**, 821 (1990).
[4] K. M. Cuomo and A. V. Oppenheim, Phys. Rev. Lett. **71**, 65 (1993); M. S. Leeson, Electron. Lett. **30**, 2014 (1994).
[5] A. E. Siegman, *Lasers* (University Science Books, Mill Valley, CA, 1986).
[6] H. G. Winful and L. Rahman, Phys. Rev. Lett. **65**, 1575 (1990).
[7] R. Roy and K. S. Thornburg, Phys. Rev. Lett. **72**, 2009 (1994).
[8] T. C. Newell, P. M. Alsing, A. Gavrielides, and V. Kovanis, Phys. Rev. Lett. **72**, 1647 (1994).
[9] T. Sugawara, M. Tachikawa, T. Tsukamoto, and T. Shimizu, Phys. Rev. Lett. **72**, 3502 (1994); Y. Liu and J. R. Rios Leite, Phys. Lett. A **191**, 134 (1994).
[10] C. L. Pando L., Phys. Lett. A **210**, 391 (1996); **223**, 359 (1996).

[11] P. Colet and R. Roy, Opt. Lett. **19**, 2056 (1994).
[12] L. D. Landau and E. M. Lifshitz, *Statistical Physics* (Pergamon, Oxford, 1978).
[13] E. Ott and J. C. Sommerer, Phys. Lett. A **188**, 39 (1994); P. Ashwin, J. Buescu, and I. Stewart, *ibid.* **193**, 126 (1994); J. F. Heagy, T. L. Carroll, and L. M. Pecora, Phys. Rev. E **52**, 1253 (1995).
[14] R. E. Amritkar and Neelima Gupte, Phys. Rev. A **44**, R3403 (1991).
[15] M. Sargent III, M. O. Scully, and W. E. Lamb, Jr., *Laser Physics* (Addison-Wesley, Reading, MA, 1974).
[16] J. C. Cotteverte, G. Ropars, A. Le Foch, and F. Bretenaker, IEEE J. Quantum Electron. **30**, 2516 (1994).
[17] V. V. Likhanskii and A. P. Napartovich, Usp. Fiz. Nauk **160**, **101 (1990) [Sov. Phys. Usp. 33**, 228 (1990)].
[18] C. Sparrow, *The Lorenz Equations: Bifurcations, Chaos and Strange Attractors* (Springer-Verlag, New York, 1982); C. O. Weiss, N. B. Abraham, and U. Hübner, Phys. Rev. Lett. **61**, 1587 (1988); C. O. Weiss, W. Klische, N. B. Abraham, and U. Hübner, Appl. Phys. B: Photophys. Laser Chem. **49**, 211 (1989); R. Vilaseca and P. Mandel, Phys. Rev. A **48**, 591 (1993), and references therein.
[19] C. L. Pando L., Opt. Commun. **116**, 94 (1995), and references therein.
[20] N. B. Abraham, P. Mandel, and L. M. Narducci, in *Progress in Optics XXV*, edited by E. Wolf (North-Holland, Amsterdam, 1988), p. 1.
[21] H. Fujisaka and T. Yamada, Prog. Theor. Phys. **74**, 918 (1985); A. S. Pikovsky, Z. Phys. B **55**, 149 (1984).
[22] C. L. Pando L., R. Meucci, M. Ciofini, and F. T. Arecchi, Chaos **3**, 279 (1993), and references therein.